

# Polysulfone and Mesoporous Molecular Sieve MCM-48 Mixed Matrix Membranes for Gas Separation

Sangil Kim and Eva Marand\*

Department of Chemical Engineering, Virginia Polytechnic Institute and State University,  
Blacksburg, Virginia 24061-0211

Junichi Ida and Vadim V. Guliants

Department of Chemical and Materials Engineering, University of Cincinnati,  
Cincinnati, Ohio 45211-0012

Received October 19, 2005. Revised Manuscript Received December 28, 2005

A mesoporous MCM-48 silica was synthesized by a templating method and mixed with polysulfone (PSF) to fabricate mixed matrix membranes (MMMs). Helium permeation data and SEM images of as-synthesized MCM-48/PSF MMMs suggest that MCM-48 silica particles adhered well to the PSF matrix and that the MMMs were defect free. Gas permeation tests indicated that the increases in permeability resulted from increases in solubility as well as diffusivity. The increases in transport properties for all tested gases make mesoporous MCM-48 silica an attractive additive for enhancing the gas permeability of MMMs without sacrificing selectivity.

## Introduction

Polymeric membranes have been very useful in addressing industrially important gas separations, thereby providing economical alternatives to conventional separation processes. However, polymeric membranes for gas separations have been known to have a tradeoff between permeability and selectivity as shown in upper bound curves developed by Robeson.<sup>1</sup> Many research efforts have been aimed at modifying the backbones and side chains of polymers experimentally to surpass the permeability-selectivity tradeoff. This has been difficult to achieve and in fact also, as shown by Freeman,<sup>2</sup> theoretically improbable. Thus, the use of polymeric materials as membranes has technical limitations.<sup>3</sup>

To enhance gas separation membrane performances, recent work has focused on enhancing polymer selectivity and permeability by fabricating mixed matrix membranes (MMMs). The incorporation of various inorganic materials, such as zeolites or carbon molecular sieves, into a polymer matrix has been investigated.<sup>4–7</sup> However, the application of zeolites is limited by the poor interaction with the polymer matrix and the relatively small zeolite pores. Transport limitations can also occur after the modification of external surfaces of zeolites with silane coupling agents, which can block pore access.<sup>8,9</sup> Weak interactions between a glassy

polymer matrix and inorganic molecular sieves may lead to the formation of nonselective voids, resulting in Knudsen flow.<sup>5</sup>

Since the discovery of the M41S family of mesoporous molecular sieves by Kresge et al.,<sup>10,11</sup> these materials have received widespread interest as catalysts, adsorbents, and membranes because of their high surface areas, tunable pore sizes (2–50 nm), and surface chemistry via functionalization. The surface of mesoporous silica is decorated with reactive silanol groups, which can be used for surface modification to introduce favorable interactions with polymers. Surface functionalization of mesoporous materials with several types of functional groups for application in adsorption and catalysis has been reported.<sup>12–16</sup> Recently, the application of these molecular sieves as membranes has been investigated by some research groups. Nishiyama et al. fabricated mesoporous MCM-48 membranes on a porous alumina support and reported that the permeation of gases through calcined MCM-48 membranes was governed by Knudsen diffusion.<sup>17,18</sup> Reid et al. reported polysulfone (PSF) MMMs with mesoporous silica MCM-41 for gas separation.<sup>19</sup> They

\* Corresponding author. Phone: (540) 231-8231; fax: (540) 321-5022; e-mail: emarand@vt.edu.

- (1) Robeson, L. M. *J. Membr. Sci.* **1991**, 62, 165.
- (2) Freeman, B. D. *Macromolecules* **1999**, 32, 375.
- (3) Koros, W. J.; Fleming, G. K. *J. Membr. Sci.* **1993**, 83, 1.
- (4) Mahajan, R.; Koros, W. J. *Ind. Eng. Chem. Res.* **2000**, 39, 2692.
- (5) Mahajan, R.; Koros, W. J. *Polym. Eng. Sci.* **2002**, 42, 1420.
- (6) Mahajan, R.; Koros, W. J. *Polym. Eng. Sci.* **2002**, 42, 1432.
- (7) Kulprathipanja, S.; Neuzil, R. W.; Li, N. United States Patent No. 4,740,219, 1988.
- (8) Pechar, T. W.; Kim, S.; Vaughan, B.; Marand, E.; Baranauskas, V.; Riffle, J.; Jeong, H. K.; Tsapatsis, M. *J. Membr. Sci.*, in press.

- (9) Pechar, T. W.; Kim, S.; Vaughan, B.; Marand, E.; Tsapatsis, M.; Jeong, H. K.; Cornelius, C. J. *J. Membr. Sci.*, in press.
- (10) Kresge, C. T.; Leonowicz, M. E.; Roth, W. J.; Vartuli, J. C.; Beck, J. S. *Nature* **1992**, 359, 710.
- (11) Beck, J. S.; Vartuli, J. C.; Roth, W. J.; Leonowicz, M. E.; Kresge, C. T.; Schmitt, K. D.; Chu, C. T. W.; Olson, D. H.; Sheppard, E. W.; McCullen, S. B.; Higgins, J. B.; Schlenker, J. L. *J. Am. Chem. Soc.* **1992**, 114, 10834.
- (12) Zhao, X. S.; Lu, G. Q. *J. Phys. Chem. B* **1998**, 102, 1556.
- (13) Feng, X.; Fryxell, G. E.; Wang, L.; Kim, A. Y.; Liu, J.; Kemner, K. M. *Science* **1997**, 276, 923.
- (14) Xu, X.; Song, C.; Andresen, J. M.; Miller, B. G.; Scaroni, A. W. *Energy Fuels* **2002**, 16, 1463.
- (15) Huang, H. Y.; Yang, R. T.; Chinn, D.; Munson, C. L. *Ind. Eng. Chem. Res.* **2003**, 42, 2427.
- (16) Kim, S.; Ida, J.; Guliants, V. V.; Lin, Y. S. *J. Phys. Chem. B* **2005**, 109, 6287.



showed that mesoporous materials offered the favorable effect of increasing the permeability of the polysulfone MMMs without decreasing its selectivity due to its good compatibility with the polymer matrix. However, their study has focused on MCM-41 silica, which has a one-dimensional pore channel structure prone to diffusion limitations and pore blockage.<sup>20</sup> Therefore, MCM-48 silica is more attractive than MCM-41 for potential applications in molecular sieves in MMM areas due to its three-dimensional interconnected cubic pore structure.

The main intent of this study was to develop and characterize novel hybrid membranes based on mesoporous MCM-48 silica dispersed inside a polymer matrix. We synthesized MCM-48 mesoporous silica by a templating method and characterized it with X-ray diffraction (XRD), pore size analysis, and field emission scanning microscopes (FESEM). The structure, the absence of defects, and the properties of MCM-48/PSF MMMs were characterized by FESEM, sorption studies, and gas permeation measurements.

### Experimental Procedures

**Synthesis of MCM-48 Silica.** Mesoporous MCM-48 silica was synthesized according to a previously published procedure.<sup>17,18</sup> In this method, the aqueous micellar solution containing a quaternary ammonium surfactant,  $C_{16}H_{33}(CH_3)_3NBr$  (CTAB, Sigma-Aldrich), NaOH, and deionized water was prepared under stirring for 1 h. Then, the solution was added to tetraethyl orthosilicate (TEOS, Alfa-Aesar Chemical). The molar composition of the mixture was 0.59 CTAB/1.0 TEOS/0.5 NaOH/61  $H_2O$ . The mixture was stirred for 90 min and transferred to an autoclave. The reaction was carried out at 363 K for 96 h. The MCM-48 silica was filtered and washed with deionized water. At this stage, the as-synthesized MCM-48 still contained organic templates. Calcined MCM-48 silica used in the fabrication of MMMs was obtained after as-synthesized MCM-48 silica was calcined in air at 723 K for 5 h. To obtain a fine MCM-48 silica particle, a combination of sonication and sedimentation was performed. Following these steps, the MCM-48 silica was vacuum-dried overnight to be used in the fabrication of MMM.

**Fabrication of PSF Membranes.** Before fabrication of membranes, PSF (UDEL P-3500, Solvay) was degassed at 413 K for 3 h under vacuum to remove adsorbed water. Then, 0.6 g of the PSF was dissolved in 3 mL of chloroform and stirred for 1 day leading to a viscous solution. The membranes were cast onto a glass substrate using a doctor blade. The glass substrate was covered with a glass cover to slow the evaporation of solvent, allowing for a film with a uniform thickness without curling. The solutions were given 1 day to dry at room temperature. Once dry, the films were placed under vacuum; the temperature was raised to the glass transition temperature of the polymer, 458 K, for 1 h and the films were then cooled to room temperature. A 6.35 cm diameter circular sample was cut from the film and used for permeation tests.

**Fabrication of MCM-48/PSF MMMs.** The fabrication procedure for the mixed matrix membranes was identical to the pure polymer membrane preparation with the additional step of incor-

porating MCM-48 silica. For 10 wt % MCM-48/PSF MMMs, approximately 0.68 g of the pure PSF was dissolved in 3 mL of tetrahydrofuran (THF) and mixed for 24 h. A predetermined mass of MCM-48 (0.078 g) was dissolved in 1 mL of THF with a small amount of PSF solution (~5 drops) and sonicated for 10 min to enable the dilute polymer solution to coat the mesoporous silica. This MCM-48 solution was added to the polymer solution, and the mixture was allowed to mix for 6 h at room temperature. Following this time period, the mixture was sonicated for 10 min, after which it was allowed to mix for 10 min. This process was repeated several times. The membranes were cast onto a glass substrate using a doctor blade. The evaporation and heat treatments for the mixed matrix membranes were identical to that of the pure polymer membrane.

**Characterization.** The powder XRD patterns of MCM-48 mesoporous silica were recorded on a Scintag Inc., XDS 2000 spectrometer using Cu K $\alpha$  radiation with a step size of 0.02 °/s. The  $N_2$  adsorption-desorption isotherms were collected at 77 K using Micromeritics ASAP 2010. The MCM-48 silica samples were outgassed prior to these measurements at 423 K overnight under  $N_2$  flow. The surface areas were calculated using the Brunauer-Emmett-Teller (BET) method, and the pore volumes and pore diameters were calculated by the Barret-Joyner-Halenda (BJH) method. FESEM (LEO 1550) was used to study the morphology of the membranes. Sorption studies were conducted by the gravimetric system (IGA-002, Hiden Isochema). For each measurement, the samples were degassed at 403 K for 10 h at  $P \leq 10^{-6}$  mbar. All tubings and chambers were also degassed by applying a vacuum ( $P \leq 10^{-6}$  mbar). The degassed samples were then cooled to the specified temperature (308 K) with a ramping rate of 1 K/min. The gases used in this research were He,  $CO_2$ ,  $O_2$ ,  $N_2$ , and  $CH_4$  with a reported purity of 99.99% and purified again by passing through a molecular sieve trap attached to the gravimetric system. The adsorption isotherms were measured by the small stepwise pressure (or concentration) change (i.e., 100 mbar ( $P \leq 1.3$  bar) and 250 mbar ( $P > 1.3$  bar)). The gravimetric sorption studies in this research were conducted at a temperature of  $308 \pm 1$  K and a pressure range of 0.01–4 bar.

Permeabilities of the polymeric and composite membranes were measured using a constant volume varying pressure apparatus. Permeability was measured directly, and the time lag method<sup>21</sup> was applied to the recorded data to determine the diffusivity coefficient. The solubility coefficient was taken as the ratio of the permeability to diffusivity coefficient.<sup>21</sup> The gases used in this research were He,  $CO_2$ ,  $O_2$ ,  $N_2$ , and  $CH_4$ . Each gas possessed a purity of 99.99% and was used as received from Air Products. The feed pressure and temperature were kept constant at 4 atm and 308 K, respectively, for all experiments. Each gas was run through a membrane 6 times, and the average results and standard deviations were recorded. Permeabilities are reported in units of Barrer (1 Barrer =  $1 \times 10^{-10}$  cm<sup>3</sup> (STP) cm/(cm<sup>2</sup> s cm Hg)).

### Results and Discussion

The powder X-ray diffraction patterns (XRD) of the calcined MCM-48 silica are shown in Figure 1. The XRD patterns displayed Bragg peaks in the  $2\theta = 1.5$ – $8^\circ$  range, which can be indexed to different  $hkl$  reflections. The XRD patterns of the as-synthesized (not shown here) and calcined mesoporous MCM-48 powders consisted of the typical reflection at  $2.7^\circ$  (211) and weak reflections at  $3.1^\circ$  (220),  $4.9^\circ$  (420), and  $5.2^\circ$  (332), which corresponded to the

- (17) Nishiyama, N.; Park, D. H.; Koide, A.; Egashira, Y.; Ueyama, K. *J. Membr. Sci.* **2001**, *182*, 235.
- (18) Nishiyama, N.; Park, D. H.; Egashira, Y.; Ueyama, K. *Sep. Purif. Technol.* **2003**, *32*, 127.
- (19) Reid, B. D.; Ruiz-Trevino, F. A.; Musselman, I. H.; Balkus, K. J.; Ferraris, J. P. *Chem. Mater.* **2001**, *13*, 2366.
- (20) Morey, M. S.; Davidson, A.; Stucky, G. D. *J. Porous Mater.* **1998**, *5*, 195.

- (21) Crank, J. *The Mathematical of Diffusion*; Oxford Press: London, 1990.



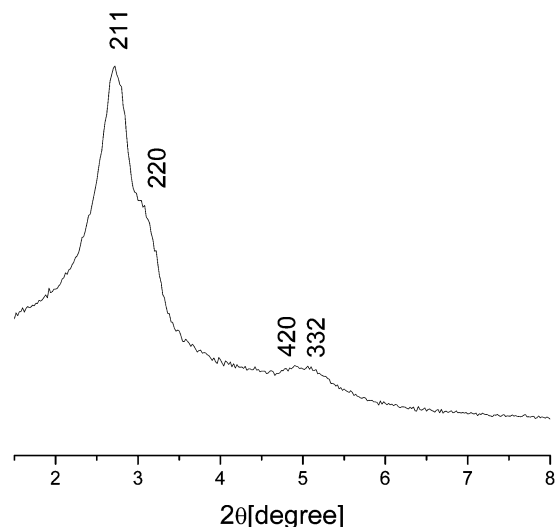


Figure 1. XRD pattern of MCM-48 silica.

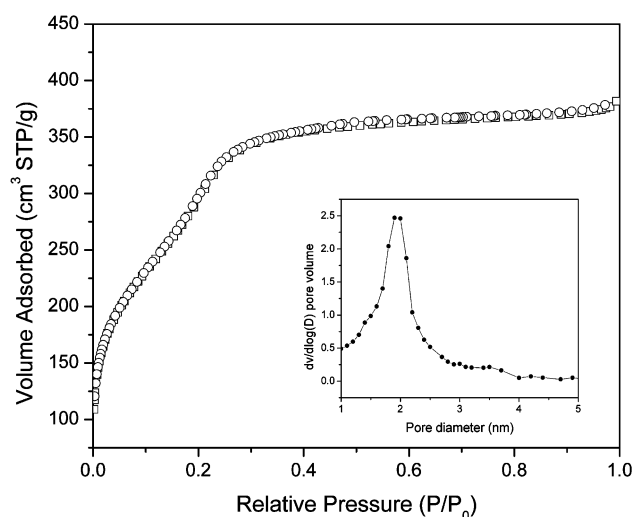


Figure 2. N<sub>2</sub> adsorption-desorption isotherms of MCM-48 silica at 77 K.

*d*-spacings of ca. 32.5, 28.7, 17.7, and 17.1 Å, respectively. These *d*-spacings are indicative of the MCM-48 structure possessing the cubic *Im3d* space group.<sup>17,18</sup> The N<sub>2</sub> adsorption-desorption isotherms at 77 K for the MCM-48 silica are shown in Figure 2. The N<sub>2</sub> adsorption isotherm of the MCM-48 is a typical reversible type IV adsorption isotherm characteristic of a mesoporous material. The MCM-48 silica had a very high surface area of around 1007 m<sup>2</sup>/g, indicating high quality. The unimodal pore size distribution is centered at 2.0 nm by the BJH method. These results are in agreement with previously published results on micellar templated mesoporous silica materials.<sup>10,11,17,18,20</sup> The FESEM images of the calcined MCM-48 particles in Figure 3 show that a narrow distribution of particle sizes ( $\sim 1 \mu\text{m}$ ) was obtained through a combination of sonication and sedimentation.

To verify the compatibility of MCM-48 silica with the glassy polymer and to check for the presence of unselective voids in the MCM-48/PSF MMMs, permeability measurements for He and O<sub>2</sub> were conducted using the PSF MMM containing 10 wt % as-synthesized MCM-48 silica (before calcinations). The external surface of uncalcined mesoporous silica is covered with electrostatically bonded surfactant molecules.<sup>22</sup> However, uncalcined mesoporous silica materi-

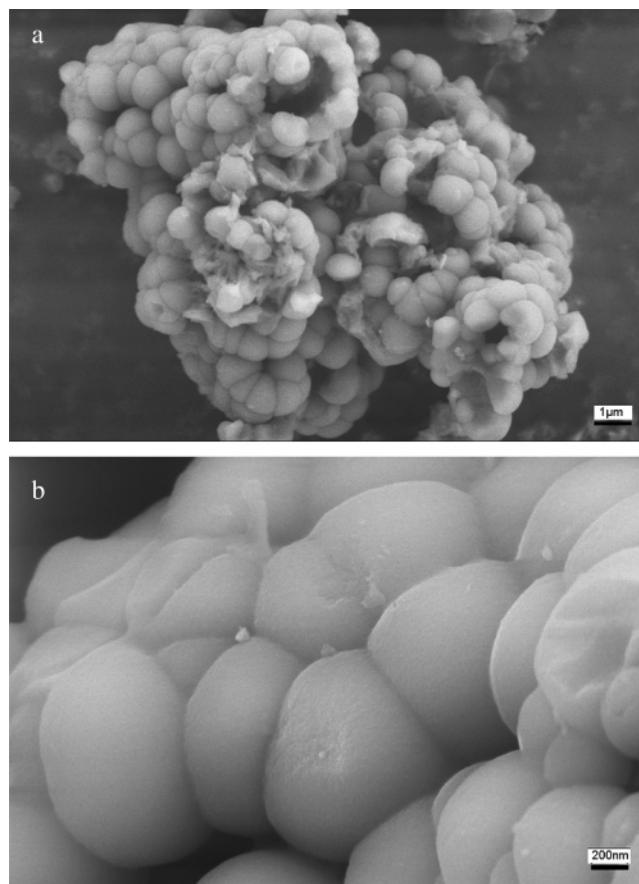


Figure 3. FESEM images of MCM-48 at (a) lower and (b) higher magnification.

Table 1. Gas Permeabilities of Pure Polysulfone and As-Synthesized MCM-48 MMMs<sup>a</sup>

wt % as-synthesized MCM-48	He	O <sub>2</sub>		
	P	P	D	S
0	8.02 ± 0.19	0.98 ± 0.06	3.33 ± 0.17	0.22 ± 0.02
10	7.98 ± 0.12	0.95 ± 0.07	3.08 ± 0.29	0.24 ± 0.01

<sup>a</sup> P = permeability, Barrer. D = diffusivity, 10<sup>-8</sup>, cm<sup>2</sup>/s. S = solubility, cm<sup>3</sup> at STP/(cm<sup>3</sup> polymer atm).

als that have been extensively washed provide external silanol groups for surface selective modifications.<sup>16,23,24</sup> Because the pores of the as-synthesized MCM-48 silica are none the less filled with organic surfactant, this silica is a good system for checking wetting properties with polymers and for the presence of defects. The presence of any unselective voids at the interface between polymer and MCM-48 should offer pathways of high permeability for helium. The He and O<sub>2</sub> permeability, O<sub>2</sub> diffusion, and solubility coefficients for PSF and 10 wt % as-synthesized MCM-48 MMM are shown in Table 1. Helium diffusion coefficients are not reported for any of the membranes in this paper. This is because the diffusion of He is fast and the time lag method introduces too much error.<sup>21</sup> Average permeabilities of He and O<sub>2</sub> dropped with the addition of MCM-48. In addition, the average diffusion coefficient of O<sub>2</sub> dropped, although its

(22) Kruk, M.; Jaroniec, M.; Sakamoto, Y.; Terasaki, O.; Ryoo, R.; Ko, C. H. *J. Phys. Chem. B* **2000**, *104*, 292.

(23) Stein, A.; Melde, B. J.; Schroden, R. C. *Adv. Mater.* **2000**, *12*, 1403.

(24) Juan, F. D.; Ruiz-Hitzky, E. *Adv. Mater.* **2000**, *12*, 430.



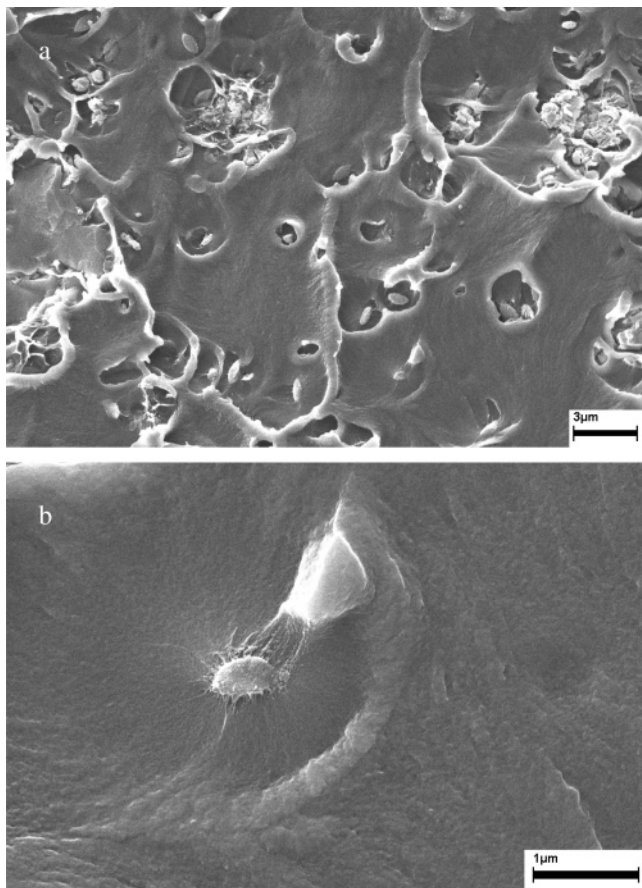


**Figure 4.** Cross-sectional FESEM images of 10 wt % as-synthesized MCM-48/PSF MMMs at (a) lower and (b) higher magnification.

solubility remained the same. This result would be consistent with the hypothesis that the as-synthesized MCM-48 silica behaves as an impermeable filler and has a good interaction with the polymer matrix.

To further investigate the presence of unselective voids in MMMs, careful FESEM inspections were carried out. FESEM cross-sectional images of 10 wt % as-synthesized MCM-48/PSF MMMs are shown in Figure 4. Figure 4a shows that MCM-48 silica particles appear to be well-dispersed throughout the PSF matrix and that few empty cavities remain representing replicas of MCM-48 silica cleaved away when the FESEM sample was prepared with liquid nitrogen. The FESEM image at higher magnification, Figure 4b, shows that the polymer adheres well to the MCM-48 silica particles and that no unselective voids are present around the mesoporous silica particles. The permeability and FESEM results suggest that as-synthesized MCM-48 added to the polymer matrix behaves as an impermeable filler, lowering the permeability of gases and hindering the diffusion of oxygen. Furthermore, MCM-48/PSF MMMs show no evidence of unselective voids.

The FESEM images of 10 to ~20 wt % calcined MCM-48/PSF MMMs are shown in Figures 5 and 6. The FESEM results of 10 wt % calcined MCM-48 loading are similar to that of the as-synthesized 10 wt % MCM-48/PSF MMMs. At 10 wt % MCM-48 loading (Figure 5a), mesoporous silica particles are well-distributed throughout the PSF matrix. Figure 5b does not show any unselective voids around calcined MCM-48 particles, suggesting better wetting prop-

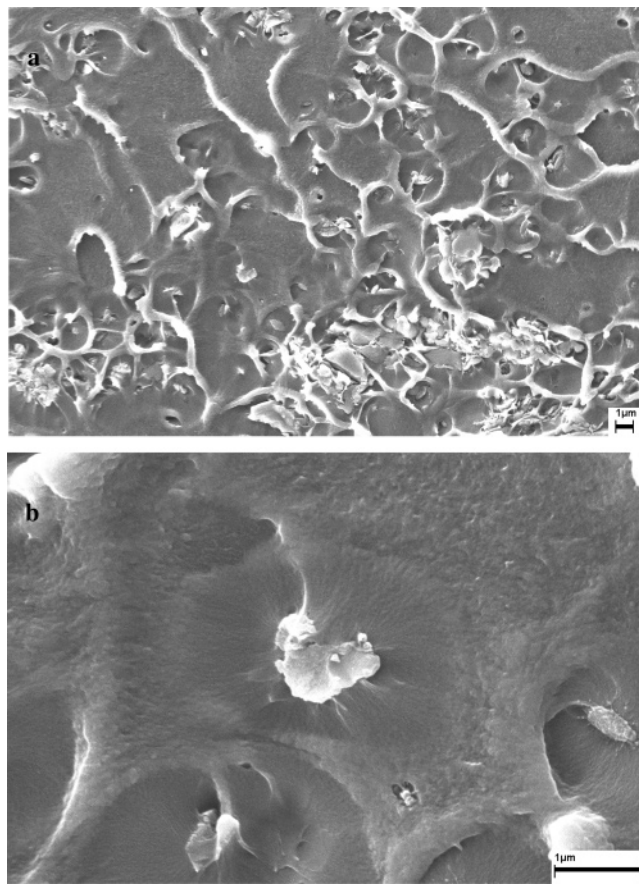


**Figure 5.** Cross-sectional FESEM images of 10 wt % calcined MCM-48/PSF MMMs at (a) lower and (b) higher magnification.

erties with the polymer matrix than is exhibited by zeolites.<sup>5,25</sup> The FESEM images of unmodified zeolites loaded in a glassy polymer matrix revealed the presence of unselective voids surrounding zeolite particles. In contrast to zeolite crystals, mesoporous MCM-48 silica particles are covered with weakly acidic surface silanol groups showing favorable interactions with organic molecules.<sup>26</sup> A reported concentration of the surface SiOH groups is about 1.8 SiOH/nm<sup>2</sup> on the MCM-48 surface.<sup>27</sup> Although this value includes both reactive single SiOH groups and also unreactive hydrogen-bonded SiOH groups, approximately one SiOH/nm<sup>2</sup> can be a primary adsorption site for other molecules.<sup>16</sup> In an ATR-FTIR spectroscopy study, Reid et al. suggested that the phenyl oxygens of PSF interact with surface silanol groups of MCM-41 silica through hydrogen bonding.<sup>19</sup> Therefore, it is possible that similar hydrogen bonding interactions occur between PSF and surface silanol groups of MCM-48, thus providing good wetting properties of MCM-48/PSF MMMs. At 20 wt % MCM-48 loadings, unlike 10 wt % loading, not all MCM-48 particles are well-distributed through the matrix, and some MCM-48 silica particles form small domains in a polymer matrix as shown in Figure 6a. Although some

(25) Duval, J.-M.; Kemperman, A. J. B.; Folkers, B.; Mulder, M. H. V.; Desgrandchamps, G.; Smolders, C. A. *J. Appl. Polym. Sci.* **1994**, *54*, 409.

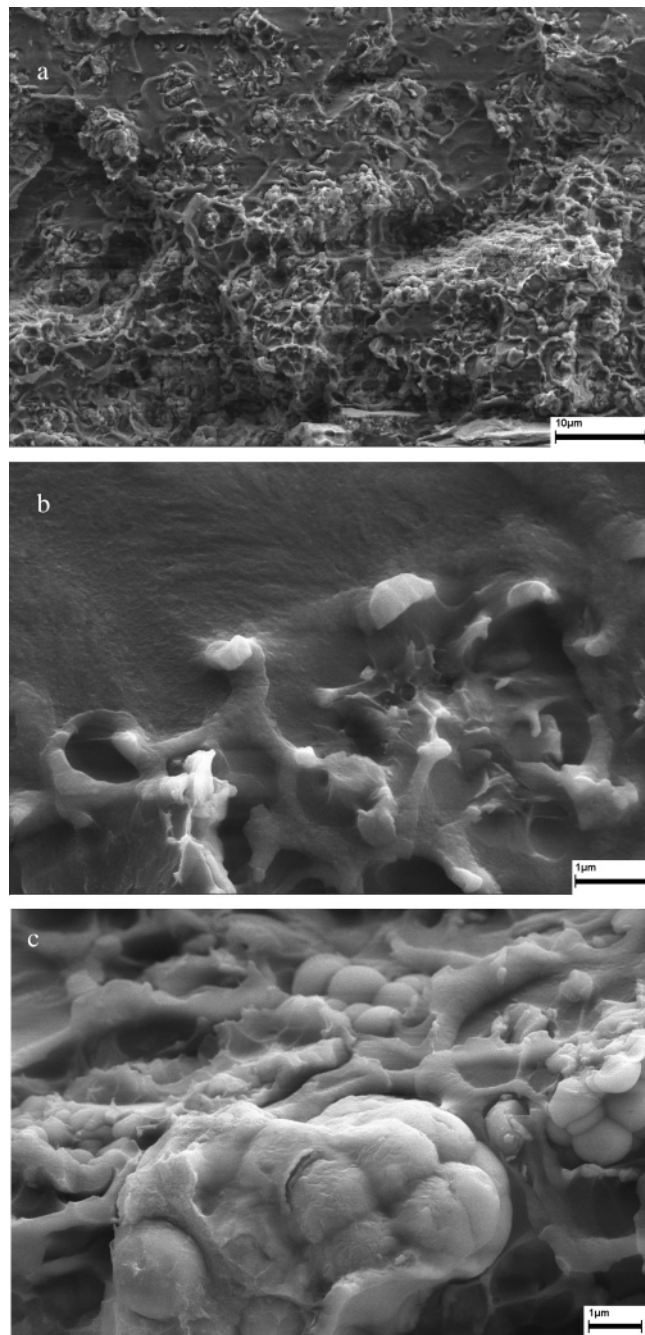
(26) Jentys, A.; Kleestorfer, K. K.; Vinek, H. *Microporous Mesoporous Mater.* **1999**, *27*, 321.

(27) Kumar, D.; Schumacher, K.; du Fresne von Hohenesche, C.; Grün, K.; Unger, K. K. *Colloids Surf., A* **2001**, *187–188*, 109.



**Table 2. Gas Permeabilities (Barrer) of Various Gases in Pure Polysulfone and MCM-48 MMMs**

membrane	MCM-48 wt %	He	CO <sub>2</sub>	O <sub>2</sub>	N <sub>2</sub>	CH <sub>4</sub>
PSF	0	8.02 ± 0.19	4.46 ± 0.10	0.98 ± 0.07	0.18 ± 0.01	0.17 ± 0.01
MCM48/PSF	10	15.75 ± 0.53 (96.38%) <sup>a</sup>	8.45 ± 0.13 (89.46%)	1.84 ± 0.10 (87.76%)	0.32 ± 0.02 (77.78%)	0.33 ± 0.02 (94.12%)
MCM48/PSF	20	32.10 ± 0.83 (300.25%)	18.21 ± 0.41 (308.30%)	4.14 ± 0.01 (322.45%)	0.77 ± 0.02 (327.78%)	0.77 ± 0.02 (352.94%)

<sup>a</sup> Increment from pure polymer.**Figure 6.** FESEM images of 20 wt % calcined MCM-48/PSF MMMs. (a) Cross-sectional view (lower magnification), (b) discontinuous phase, and (c) continuous silica phase (higher magnification).

MCM-48 particles aggregate and form silica domains, higher magnification of the FESEM image in Figure 6b,c shows that isolated silica particles and the small domains of silica particles are well-coated with the polymer.

The permeability results and ideal separation factors for the mesoporous MCM-48 silica and PSF MMMs are shown

**Table 3. Selectivity for Polysulfone and MCM-48 MMMs**

membrane	MCM-48 wt %	He/CH <sub>4</sub>	CO <sub>2</sub> /CH <sub>4</sub>	O <sub>2</sub> /N <sub>2</sub>
PSF	0	46.52	25.88	5.47
MCM48/PSF	10	47.78	25.47	5.75
MCM48/PSF	20	41.56	23.58	5.38

in Tables 2 and 3, respectively. Because of different polymer processing and film preparation history, our permeability values for pure PSF membranes are somewhat lower than those previously reported by other research groups.<sup>19,28</sup> For all tested gases (He, CO<sub>2</sub>, O<sub>2</sub>, N<sub>2</sub>, and CH<sub>4</sub>), the permeability values increased in proportion to the amount of MCM-48 silica in the polymer matrix. The addition of 10 wt % MCM-48 to PSF resulted in a ~85% increase in the permeability of all gases tested. These overall increases in permeability maintained the selectivity constant or only slightly changed as shown in Table 3. At 20 wt % MCM-48 silica loading, the permeability increased dramatically by ~300% for He and CO<sub>2</sub> and ~320% for O<sub>2</sub>, N<sub>2</sub>, and CH<sub>4</sub>. Despite these increases in permeability, the separation factor decreased only slightly or remained virtually unchanged. From the FESEM images at 20 wt % MCM-48 loading, MCM-48 silica particles form small domains throughout the polymer matrix. Koros et al. suggested that higher membrane performance can be achieved if the mixed matrix membrane morphology forms some continuous pathways through the filler component.<sup>29</sup> Some semblance of silica domain continuity can be seen in Figure 6 for the MCM48/PSF MMMs. Figure 7 illustrates simplistic, discontinuous, and continuous penetrant pathways through the molecular sieving phase of MMMs. The continuous pathways present in the polymer matrix with the addition of 20 wt % MCM-48 allow the gas molecules to diffuse solely through the molecular sieve phase such that high gas permeation performance results, while in the discontinuous phase as in the case of 10 wt % silica loading, gas molecules are forced to diffuse through the less-permeable PSF region.

The differences in permeabilities of each MMMs can be better understood by analyzing the contributions of diffusivity and solubility coefficients to the overall permeabilities. The diffusivity and solubility coefficients for the tested gases are shown in Table 4. Similar to the observed increase in permeability, after the incorporation of MCM-48 silica to the polymer, diffusivity and solubility coefficients for all tested gases increased monotonically. Increases in gas permeability have been reported for polymer/silica MMMs.<sup>19,30–32</sup> The increases in the O<sub>2</sub>/N<sub>2</sub> selectivity and

(28) Gür, T. M. *J. Membr. Sci.* **1994**, 93, 283.

(29) Zimmerman, C. M.; Singh, A.; Koros, W. J. *J. Membr. Sci.* **1997**, 137, 145.

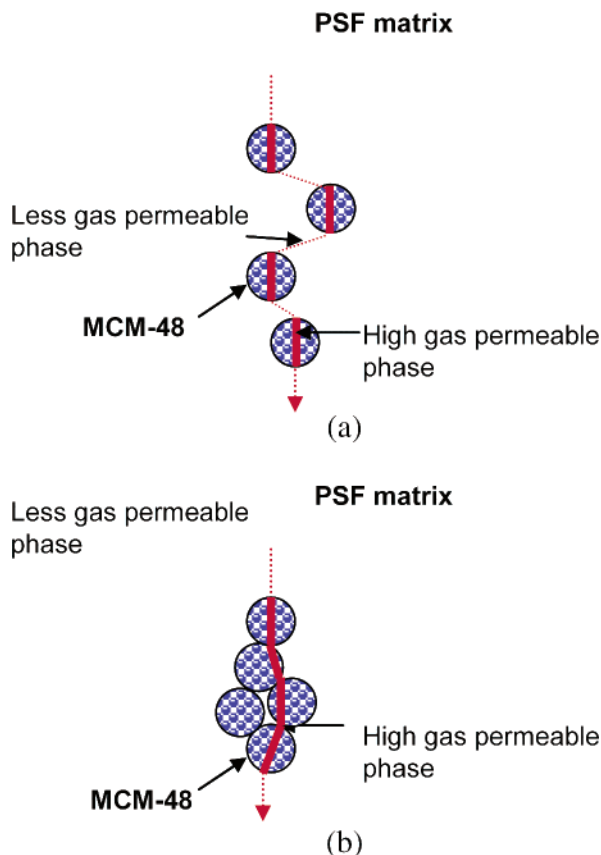
(30) Merkel, T. C.; Freeman, B. D.; Spontak, R. J.; He, Z.; Pinnau, I.; Meakin, P.; Hill, A. J. *Chem. Mater.* **2003**, 15, 109.



Table 4. Diffusivity (D) and Solubility (S) of Various Gases in Pure Polysulfone and MCM-48 MMMs<sup>a</sup>

membrane	CO <sub>2</sub>		O <sub>2</sub>		N <sub>2</sub>		CH <sub>4</sub>	
	D	S	D	S	D	S	D	S
PSF	1.11 ± 0.01	3.06 ± 0.07	3.33 ± 0.17	0.22 ± 0.02	1.05 ± 0.12	0.13 ± 0.01	0.26 ± 0.01	0.50 ± 0.03
10 wt % MCM48/PSF	2.06 ± 0.04	3.11 ± 0.07	5.03 ± 0.34	0.28 ± 0.00	1.35 ± 0.04	0.18 ± 0.01	0.44 ± 0.03	0.57 ± 0.03
20 wt % MCM48/PSF	3.00 ± 0.03	4.61 ± 0.06	6.75 ± 0.11	0.47 ± 0.01	1.40 ± 0.25	0.42 ± 0.06	0.48 ± 0.02	1.21 ± 0.06

<sup>a</sup> D = 10<sup>-8</sup>, cm<sup>2</sup>/s. S = cm<sup>3</sup> at STP/(cm<sup>3</sup> polymer atm).



**Figure 7.** Simple illustration for (a) discontinuous pathway through MCM-48 (10 wt % MCM-48 loading) and (b) continuous pathway through MCM-48 (20 wt % MCM-48 loading).

oxygen permeability as compared to those in a pristine polymer were observed for the polymer/silica composites by Koros et al.<sup>32</sup> The increase in permeability was attributed to the disruption of polymer chain packing in the presence of the silica particles.<sup>32</sup> Also, Freeman et al. suggested that nanometer-sized fumed silica (FS) particles are able to disrupt the packing of rigid polymer chains, thereby subtly increasing the free volume available for molecular transport.<sup>30</sup> For example, at 20 wt % FS loading, methane permeability in the FS-filled glassy polymer is approximately 140% higher than that in the pure polymer membrane. The increase in permeability of MCM-48/PSF MMMs observed here is more than twice that of the FS-filled polymer membrane system, suggesting that some permeation also occurs through the MCM-48 pores. The pore size of the tested MCM-48 silica is 2.0 nm by the BJH method. However, the BJH method overpredicts the pressures of the capillary condensation/desorption and thus underestimates the calculated pore size

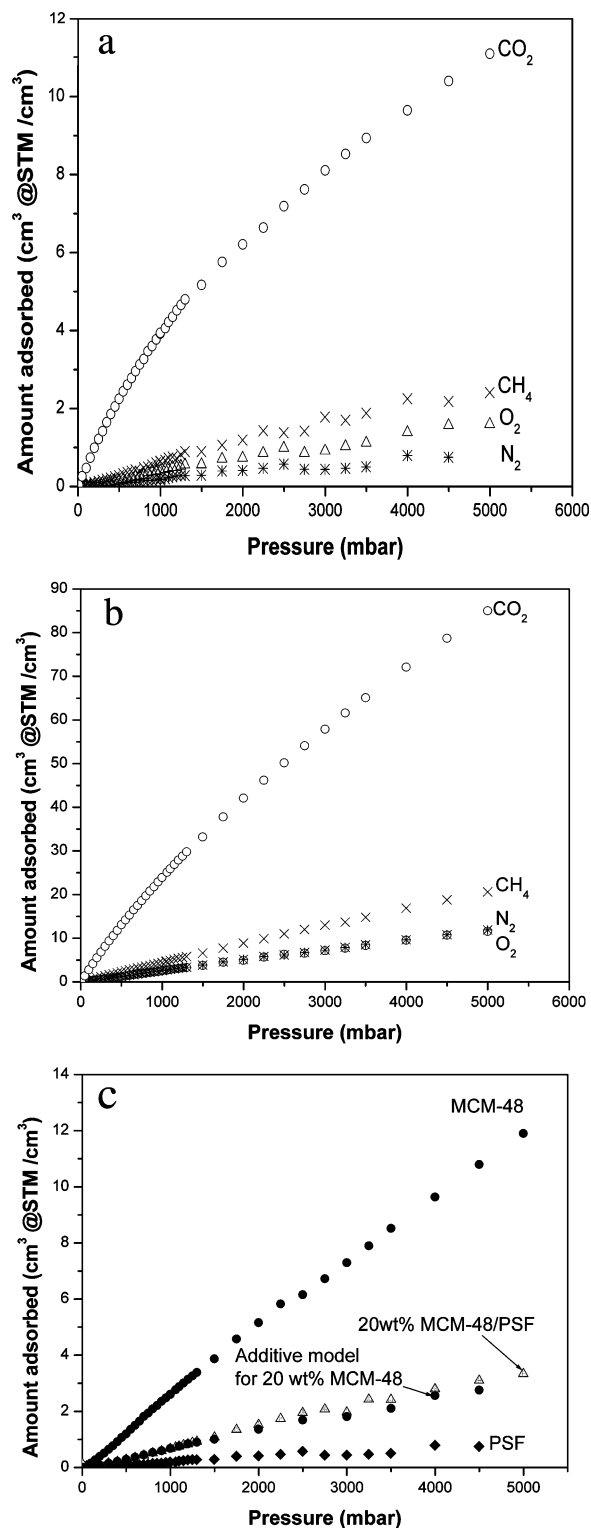


**Figure 8.** Gas adsorption isotherms for (a) PSF, (b) MCM-48 silica, and (c) 20 wt % MCM-48/PSF MMMs for N<sub>2</sub>.

in typical mesoporous silica materials by ca. 1.0 nm or by 25–30% as the pore size approaches 2.0 nm.<sup>22,33,34</sup> Thus,

(31) Merkel, T. C.; He, Z.; Pinnau, I.; Freeman, B. D.; Meakin, P.; Hill, A. J. *Macromolecules* **2003**, *36*, 8406.

(32) Moaddeb, M.; Koros, W. J. *J. Membr. Sci.* **1997**, *125*, 143.



the MCM-48 silica pore size should be near 3.0 nm. While this may enhance gas diffusion, the pore openings may not be large enough to enable penetration of the high molecular weight polymer. Therefore, the monotonic increase in diffusivity could be a consequence of the presence of high diffusivity tunnels and redistribution of the rigid polymer chain near the pore entrance. As shown in Table 4, the solubility coefficients also increase with the addition of MCM-48 silica. To better explain the increases in solubility in the MCM-48/PSF MMMs system, separate sorption studies for MCM-48, PSF, and MMMs were carried out. These gas sorption isotherms are shown in Figure 8. As shown in Figure 8a,b, mesoporous MCM-48 silica has a higher adsorption capacity than PSF because of its high coverage of silanol groups on the silica surface.<sup>16,26,27</sup> For porous filler particles dispersed in a continuous polymer matrix, the solubility of the composite can be modeled by<sup>31</sup>

$$S = \phi_{\text{MCM48}} S_{\text{MCM48}} + (1 - \phi_{\text{MCM48}}) S_{\text{PSF}} \quad (1)$$

where  $S_{\text{MCM48}}$  and  $S_{\text{PSF}}$  are the intrinsic solubilities of MCM-48 and PSF. The volume fraction of MCM-48 ( $\phi_{\text{MCM48}}$ ) has been estimated using pure component densities as follows:<sup>31</sup>

$$\phi_{\text{MCM48}} = \frac{w_{\text{MCM48}}}{w_{\text{MCM48}} + \frac{\rho_{\text{MCM48}}}{\rho_{\text{PSF}}}(1 - w_{\text{MCM48}})} \quad (2)$$

Here,  $\rho_{\text{MCM48}}$  and  $\rho_{\text{PSF}}$  denote the MCM-48 silica and pure polymer densities, respectively, and  $w_{\text{MCM48}}$  is the silica weight fraction. The densities of MCM-48 and PSF used here were 1.64 and 1.24 g/cm<sup>3</sup>, respectively.<sup>35</sup> The calculated and experimental value of the solubility coefficients of N<sub>2</sub> at 4 bar and 308 K are shown in Table 5. The addition of 20 wt % MCM-48 silica resulted in a 255% increase in the solubility of N<sub>2</sub> (0.20 to 0.71 cm<sup>3</sup> at STP/(cm<sup>3</sup><sub>polymer</sub> atm)). In Figure 8c, the predicted N<sub>2</sub> uptake for PSF containing 20 wt % MCM-48 based on the pure material sorption capacities and the additive model are expressed by eq 1. The measured uptake by 20 wt % MCM-48/PSF MMM shows a very

**Table 5. Calculated and Experimental Solubility Coefficients of N<sub>2</sub> at 4 Bar**

	solubility coefficients, cm <sup>3</sup> at STP/(cm <sup>3</sup> <sub>polymer</sub> atm)
	N <sub>2</sub>
PSF	0.20
MCM48	2.44
20 wt % MMM	0.71
calculated 20 wt % MMM	0.65

similar trend with the gas sorption values predicted by the additive model. Table 5 shows that the experimental solubility coefficient of MMM containing 20 wt % MCM-48 (0.71 cm<sup>3</sup> at STP/(cm<sup>3</sup><sub>polymer</sub> atm)) corresponds to the theoretical value (0.65 cm<sup>3</sup> at STP/(cm<sup>3</sup><sub>polymer</sub> atm)). Therefore, the increase in permeability of MCM-48/PSF MMMs can be attributed to an increase in diffusivity as well as solubility.

## Conclusion

Mixed matrix membranes were prepared using a mesoporous MCM-48 silica synthesized by a templating method and a polysulfone as the polymer matrix. The high surface coverage of silanol groups on MCM-48 provided good interaction with the PSF matrix. Helium permeation data and SEM images of as-synthesized MCM-48/PSF MMMs suggest that MCM-48 silica particles adhered well to PSF and that prepared MMMs were defect free. Mesoporous MCM-48 materials offer the favorable effect of a large increase in gas permeability in MMMs without sacrificing selectivity. These dramatic increases in gas permeability resulted from increases in solubility as well as diffusivity. The continuous pathways present in the polymer matrix with the high loading of MCM-48 silica allowed the gas molecules to diffuse solely through the molecular sieve phase such that high gas permeation performance results. The measured uptake of MCM-48/PSF MMM showed a very similar increase in the gas sorption capacities predicted by a simple theoretical model. The observed increases in both diffusivity and solubility make mesoporous MCM-48 silica an attractive additive for enhancing the gas permeability of MMMs without sacrificing selectivity.

**Acknowledgment.** The authors gratefully acknowledge Solvay Advanced Polymers for kindly providing the polysulfone (P-3500) used in this study. We thank Benjamin R. Vaughan who collected XRD data and Steve McCartney for his help with the FESEM images.

CM0523050

(33) Ravikovitch, P. I.; Wei, D.; Chueh, W. T.; Haller, G. L.; Neimark, A. V. *J. Phys. Chem. B* **1997**, *101*, 3671.

(34) Ravikovitch, P. I.; Neimark, A. V. *Langmuir* **2000**, *16*, 2419.

(35) Innocenzi, P.; Martucci, A.; Guglielmi, M.; Bearzotti, A.; Traversa, E.; Pivin, J. C. *J. Eur. Ceram. Soc.* **2001**, *21*, 1985.